New radiation-tolerant thin planar and 3D columnar n^+ on p silicon pixel sensors

M. Boscardin[1], R. Ceccarelli[2], G.F. Dalla Betta[3], G. Darbo[4], M.E. Dinardo[5], G. Giacomini[6], D. Menasce[7], R. Mendicino[3], M. Meschini[8], A. Messineo[9], L. Moroni[7], R. Rivera[10], S. Ronchin[6], D.M.S. Sultan[3], L. Uplegger[10], L. Viliani[2], I. Zoi[11], D. Zuolo[5].

***Abstract*—The High Luminosity upgrade of the CERN Large Hadron Collider (HL-LHC) calls for a new high radiation-tolerant solid-state pixel sensor, capable of surviving irradiation fluences up to a few 10^{16} n_{eq}/cm^2 at $\sim$ 3 cm from the interaction point. The INFN ATLAS-CMS joint research activity, in collaboration with Fondazione Bruno Kessler, is aiming at the development of thin n^+ on p type pixel sensors to be operated at the HL-LHC. The R&D covers both planar and 3D pixel devices made with the Direct Wafer Bonding technique. The active thickness of the planar sensors is 100 μm or 130 μm, that of 3D sensors 130 μm only. First prototypes of hybrid modules, bump-bonded to the present CMS readout chips, have been characterized in beam tests. First results on their performance before and after irradiation are reported in this article.**

***Index Terms*—pixel, Silicon, sensor, planar, 3D, radiation hard, HL-LHC**

I. Introduction

The two general purpose experiments at the CERN Large Hadron Collider (LHC) [1], ATLAS [2] and CMS [3], will undergo a major upgrade in order to cope with the High Luminosity program of the LHC (HL-LHC). In particular, the pixel detector of the CMS experiment is designed to be located at $\sim$ 3 cm from the interaction point. At such a close distance, the 1-MeV neutron equivalent fluence, after 3000 fb^{-1} of delivered lumi, i.e. after ten years of operation, is expected to reach 2.3×10^{16} n_{eq}/cm^2. The design of planar silicon detectors currently used in CMS is ultimately limited by the degradation of the signal-to-noise ratio and it can be reliably employed up to few 10^{15} n_{eq}/cm^2. Therefore, a new high-radiation tolerant solid-state pixel sensor design, capable to withstand ten times this fluence, needs to be developed. One of the most critical geometrical parameters in the development of these sensors is the distance between the electrodes that generate the electric field for charge collection. It is well known that in order to operate these sensors at higher irradiation fluences, the input of the pre-amplifier should be connected to the electrode which collects electrons (the faster carriers). Furthermore, in order to keep the bias voltage as low as possible while preserving the largest part of the signal, the distance between opposite sign electrodes should not exceed few times the electrons mean-free-path at saturation velocity.

The best choice is a n^+ on p sensor which avoids type-inversion of the bulk and is less expensive since it allows for a single-sided process[1].

In the considered HL-LHC scenario, the expected electron lifetime becomes ~ 0.3 ns and the mean-free-path, at saturation velocity, ~ 30 μm [4] (the mean-free-path of the holes is shorter, hence their contribution to the signal is even smaller).

Two different technological solutions are available: planar sensors, where the electrodes are parallel to the sensor surface, and 3D sensors, where the electrodes are orthogonal to the sensor surface. In the first case the distance between the electrodes is fixed by the sensor's active layer thickness, in the second case it is limited by the layout and the technological process used to build the sensor.

To keep the pixel occupancy at per mil level at the expected HL-LHC peak luminosity of $7.5 \times 10^{34} cm^{-2} s^{-1}$, and to improve the spatial resolution, the foreseen pixel cell size is of 25×100 μm^2 or 50×50 μm^2 [5].

A joint ATLAS-CMS INFN group is collaborating with the Fondazione Bruno Kessler-FBK foundry (Trento, Italy), to develop thin planar and 3D Silicon pixel sensors on n^+ on p 6" Float Zone (FZ) wafers, employing a recent technology, called Direct Wafer Bonding (DWB). In the present case, a high resistivity p-type wafer is directly bonded with a low resistivity p^+ wafer. The former constitutes the active part of the sensor, while the latter provides mechanical support and Ohmic contact for the other wafer [6].

In this article, we will present test beam results on the performance of such sensors before and after irradiation up to the maximal fluence tolerated by the employed readout chips, $\sim 5 \times 10^{15}$ n_{eq}/cm^2.

II. Sensor description

The dimensions and granularity of the present prototype sensors are designed to be compatible with the readout chip we used for tests, namely, the PSI46 digital chip [7], currently employed in CMS and consisting of a matrix of 80 rows and 52 columns of 100×150 μm^2 pixels.

[1] Fond. Bruno Kessler, Povo and TIFPA-INFN, Trento - Italy
[2] Firenze U. and INFN, Firenze - Italy
[3] Trento U. and TIFPA-INFN, Trento - Italy (now with Geneva U.)
[4] INFN, Genova - Italy
[5] Milano-Bicocca U. and INFN, Milano-Bicocca - Italy
[6] Fond. Bruno Kessler, Povo - Italy
[7] INFN, Milano-Bicocca - Italy
[8] INFN, Firenze - Italy
[9] Pisa U. and INFN, Pisa - Italy
[10] Fermi National Accelerator Laboratory, Batavia - USA
[11] Hamburg U., Hamburg - Germany

[1] In this case, both the pixel implants and the guard-ring structure are on the same side.

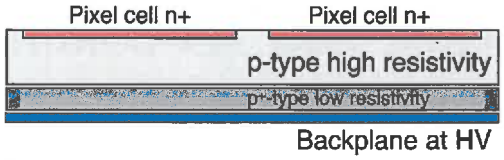

Fig. 1. Sketch showing the cross section of a thin planar n^+ on p sensor. The thickness of the high resistivity layer (i.e. active layer) can be 100 or 130 μm, while that of the low resistivity layer can range from 185 to 50 μm. The two layers are bonded together with the Direct Wafer Bonding technique [6].

The thin planar sensors (Fig. 1) are produced with two nominal active layer thicknesses, 100 and 130 μm. The measured thickness is about 10 μm smaller than nominal due to Boron diffusion from the underlying p-type layer [8]. Therefore the expected Most Probable Value (MPV) for the signal released by an orthogonally incident Minimum Ionizing Particle (MIP) should be about 6351 e^- and 8740 e^- for 100 and 130 μm thick sensors respectively [9]. The pixel cell dimensions are 100×150 μm^2 as those of the readout chip. Some sensors have been fabricated with bias punch-through structures, as shown in Fig. 2, to investigate their impact on performance.

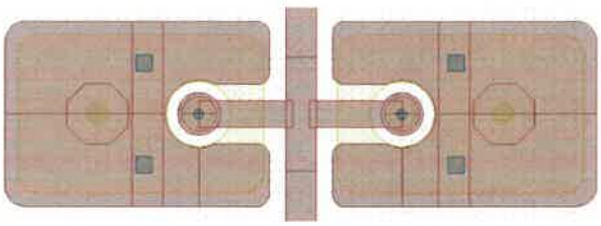

Fig. 2. The drawing of the bias punch-through structure. The bias line runs between two adjacent pixel columns and biases the punch-through dots of the nearby pixel cells.

Several variants of pixel isolation techniques are implemented. They can be p-spray only or p-spray with p-stop. In addition, the p-spray concentration can be Low, Medium and High[2], while the p-stop rings can be Open or Close. To properly characterize the isolation performance of these structures, the sensors should be irradiated at much higher fluence than those quoted in this paper. In fact, we can anticipate that in our tests of irradiated sensors we do not observe any anomaly, which can be attributed to lack of pixel isolation.

The 3D Silicon sensors are made with a single-sided process, optimized by FBK [8] and sketched in Fig. 3. Two types of columnar electrodes are implemented: p^+ Ohmic columns, which terminate in the underlying layer (i.e. the low resistivity one) in order to be biased, and n^+ junction columns, which end $\sim$ 20 μm before the low resistivity layer. The nominal column diameter is, for both junction and Ohmic columns, $\sim$ 5 μm.

Sensor modules are produced with three different pixel sizes and different numbers of junction/Ohmic columns [10].

[2]The actual p-spray concentrations are subjected to nondisclosure agreements.

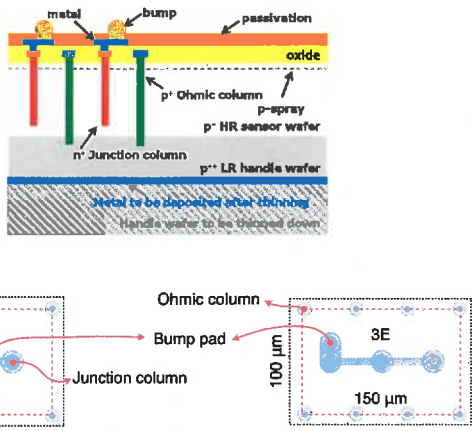

Fig. 3. The top figure provides the sketch of the production process of the 3D Silicon pixel sensors by Fondazione Bruno Kessler (Trento, Italy) [8]. Sensor modules are produced with a high resistivity layer (i.e. active layer) thickness of 130 μm, and with a low resistivity layer thickness of $\sim$ 500 μm. The two layers are bonded together with the Direct Wafer Bonding technique [6]. The layouts of the 100×150 μm^2 pixel cells with two (2E, left) and three (3E, right) junction columns are shown at the bottom. The Ohmic columns are in light green at the periphery of the pixel cells.

Standard sensors, i.e. those with 100×150 μm^2 pixel size and therefore fully compatible with the readout chip, come in two flavors: with three and two junction columns, Fig. 3. By convention, these two types of pixel cells are called 3E and 2E respectively, where E stays for readout Electrodes. The non-standard sensors, instead, can have a 50×50 μm^2 or 25×100 μm^2 pixel size and their cell structure is, respectively, of type 1E and 2E. In each cell the bump pad is typically located next to one of the junction columns except for a variant of the 25×100 μm^2 sensor for which it is on the top of a junction column. This is to free space between the junction and Ohmic columns thus reducing the risk of short circuits. While standard sensors can be fully read out, only one sixth of the pixels of the other sensors can be read out. In addition this requires a pitch adapter to match the readout-chip input pad and a special circuit to bias the other pixels that are not read out (Fig. 4).

III. Test Beam Setup, Readout Electronics, and Data Analysis

Test beam studies, both of thin planar and 3D devices, have been performed at the Fermilab Test Beam Facility with a 120 GeV proton beam.

The beam particle trajectories are reconstructed by means of a telescope of 8 planes of the same pixel detectors employed in the first running phase of CMS (PSI46 analog chip [3], with 100×150 μm^2 pixel cell size, 80 rows and 52 columns). The track extrapolation error at the center of the telescope, where the detectors under test (DUTs) are placed, is $\sim$ 8 μm on both transverse coordinates. The Data Acquisition system (DAQ) is based on CAPTAN [11] boards which read out all telescope planes together with the DUTs.

The DUTs are kept at a constant temperature by means of a cooling system, based on a water-glycol chiller and an

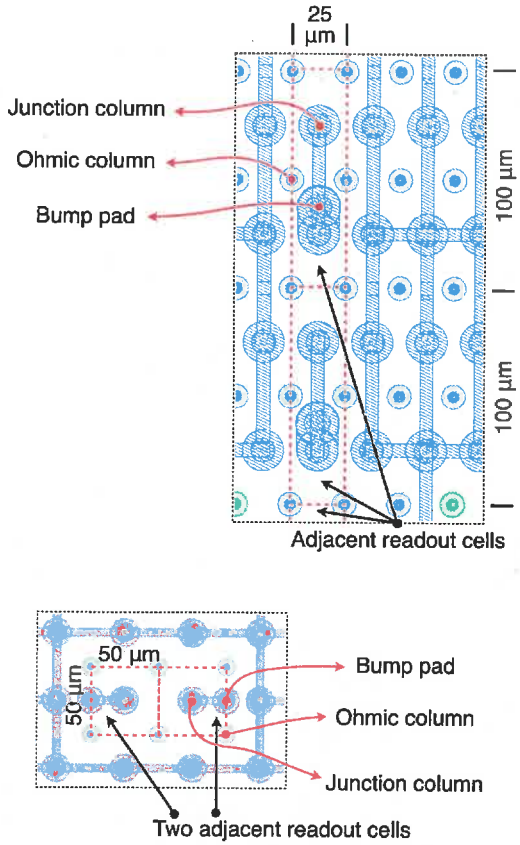

Fig. 4. Layout of the 25×100 μm^2 (top figure) and 50×50 μm^2 (bottom figure) pixel sizes. The Ohmic columns are shown in light green at the periphery of the cells.

additional set of Peltier cells. Before irradiation, the sensor modules are kept at room temperature, while, after irradiation, the temperature is set to $-20°$ C.

The track reconstruction and the detector alignment are performed by means of the Monicelli code [11]. The tracks used for the measurement of the DUT performance are selected with the following criteria:

- no more than one track in an event;
- the tracks must have an associated hit on each telescope plane;
- no more than 5 hits on each plane;
- the track χ^2 / d.o.f. must be smaller than 5.

The charge collection performance of the DUTs is investigated through the measured spectra of the MIP signal released by othogonally incident beam particles. For standard sensors, i.e. those having the same granularity as the readout chip, 100×150 μm^2 pixel size, the MIP signal is measured selecting events with an isolated hit, for which the track impact point is within a fiducial area of the pixel, 20 μm away from its boundaries. For finer pixel sensor sizes, namely 50×50 μm^2 and 25×100 μm^2, the fiducial area cut is not applied since it would exclude 96% of the events in the first case and the totality in the other. The distribution of the charge signals is then fitted with a convolution of a Landau and a Gaussian function. The returned MPV of the Landau function (hereafter referred to as MIP-MPV) is affected by a systematic error of about 5% due to charge calibration circuitry of the readout chip. This error is evaluated demanding statistical consistency ($\chi^2 = 1$) of a sample of MIP-MPVs as measured in each quadrant of a sensor and for several sensors.

The detection efficiency of the DUTs is measured by requiring that the pixel pointed to by the track, or at least one of its eight neighboring cells, be above threshold.

The irradiation of the sensor modules was performed at two facilities: at Los Alamos with 800 MeV protons [12], up to $\sim 1.2 \times 10^{15}$ n_{eq}/cm^2, and at CERN IRRAD with 24 GeV protons [13], up to $\sim 5 \times 10^{15}$ n_{eq}/cm^2. The irradiation was performed without any cooling and with sensors bump bonded to the readout chip and unpowered. After the irradiation the detectors have been constantly kept in a refrigerator at $-20°$ C to avoid important annealing effects. Due to the limited radiation resistance of the PSI46 chip ($\sim 5 \times 10^{15}$ n_{eq}/cm^2), the sensors couldn't be exposed to higher irradiation fluences. To test the sensors up to the expected fluence at HL-LHC we will use, once available, the first prototype of the RD53 chip [14] (joint ATLAS-CMS collaboration to develop a highly radiation-tolerant readout chip, in 65 nm CMOS technology, for the HL-LHC), which will feature a 50×50 μm^2 granularity.

IV. Performance of Thin Planar Sensors

Figure 5 shows the MIP-MPV as a function of the bias voltage for two couples of non-irradiated sensors of different thickness. The charge collected by the non-irradiated sensors matches the expectations. The measured particle detection efficiency is typically around 98% for sensors with a bias punch-through structure and 99.8% for the others.

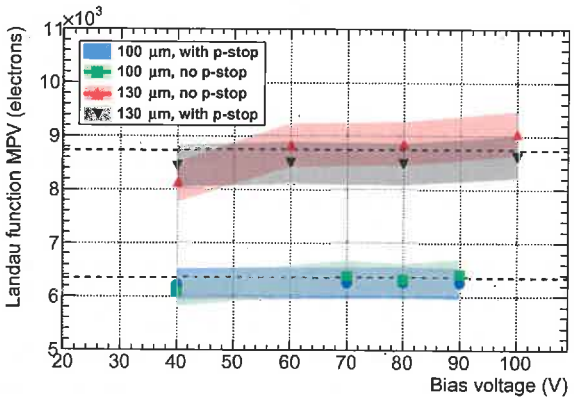

Fig. 5. MIP-MPV as a function of the bias voltage for non-irradiated thin planar sensors. The pixel size is 100×150 μm^2. The dashed lines reflect the uncertainty of the measurements and the dashed lines denote their expected values.

Figure 6 (top) shows the MIP-MPV as a function of bias voltage for three sensors irradiated up to different fluences. At the maximum fluence of $\sim 5 \times 10^{15}$ n_{eq}/cm^2 and 650 V bias voltage, the 100 μm thickness sensor reaches more than 90% charge collection efficiency (charge collection efficiency

is the ratio between the measured MIP-MPV in electrons and the expected one in absence of carrier-trapping, i.e. 6351 e^- for the thinner sensors and 8740 e^- for the others). At the intermediate fluence of $\sim 3 \times 10^{15}$ n_{eq}/cm^2, the other 100 μm thickness sensor reaches full charge collection efficiency at about 500 V, while, at the same bias voltage and less than half fluence, the thicker sensor is still loosing an important fraction of the charge, about 21%.

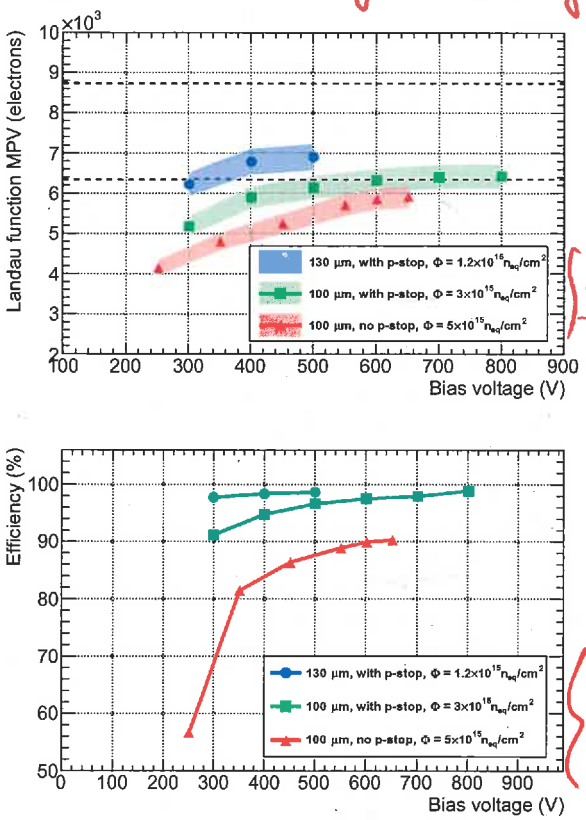

Fig. 6. MIP-MPV (top plot) and particle detection efficiency (bottom plot) as a function of the bias voltage for irradiated thin planar sensors. The sensors have bias punch-through structures except the one at the intermediate fluence. The dashed lines in the top plot reflect the uncertainty of the measurements and the dashed lines denote their expected values.

The measured MIP signal spectra, at the highest bias-voltages applied to each sensor, are shown in Figure 7. They are corrected to account for the main factors affecting the calibration circuit of the readout chip when operated at high radiation doses, i.e. the variation of the bandgap reference-voltage [15] and the change of the amplifier gain at high sensor leakage-current of the order of hundreds of μA.

The measured particle detection efficiency for the same irradiated sensors is shown at the bottom of Fig. 6. For the following discussion, it is important to keep in mind that the sensors have punch-through structures except the one at the intermediate fluence. The detection efficiency of the sensor irradiated up to $\sim 5 \times 10^{15}$ n_{eq}/cm^2 doesn't exceed $\sim 90\%$ for two reasons: the relatively high threshold set in the readout chip (in order to mitigate the noise hit-rate, we have to set the

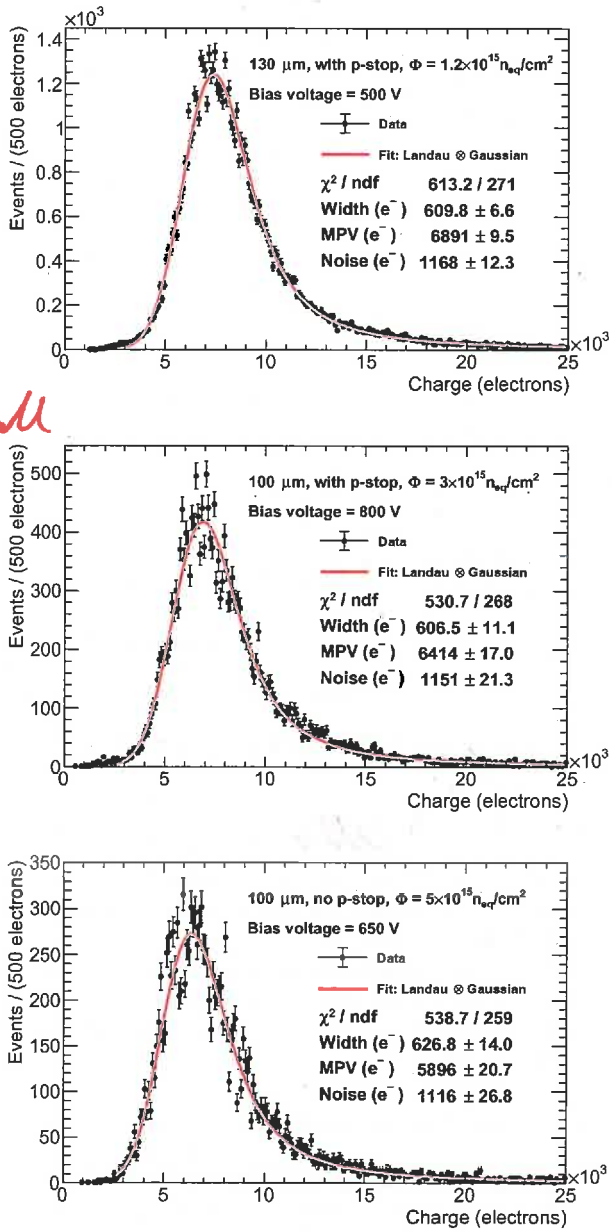

Fig. 7. MIP signal spectra at the highest bias-voltages applied to each sensor of Fig. 6: sensor irradiated up to $\sim 1.2 \times 10^{15}$ n_{eq}/cm^2 (top), sensor irradiated up to $\sim 3 \times 10^{15}$ n_{eq}/cm^2 (center), and sensor irradiated up to $\sim 5 \times 10^{15}$ n_{eq}/cm^2 (bottom). The applied bias voltage is 500 V, 800 V, and 650 V, respectively. Superimposed on each spectrum is its best fit performed with a convolution of a Landau and a Gaussian function. The main parameters returned by the fit are reported on the plot: Width: Landau natural width; MPV: Landau Most Probable Value; Noise: Gaussian rms.

threshold at around 2800 electrons) and the bias punch-through structure, which can cause a loss of efficiency from 2% up to 6% depending on the bias voltage and irradiation. Indeed, if we limit the calculation of the efficiency only to the half-cells without punch-through structures, we obtain a detection efficiency of 96.4% at 650 V bias voltage. To better illustrate this effect, we report in Fig. 8 the maps of the detection efficiency within the pixel cells of the same sensor before irradiation at bias voltages of 40 V (top plot) and 150 V (center plot), and, once irradiated, at a bias of 650 V (bottom plot). The inefficiency, initially limited only to the punch-through dot region, at higher bias voltage starts to affect also the region of the bias grid and, finally, at much higher bias voltage and after the irradiation, it extends to the whole area of the bias grid. The observed loss in efficiency is practically independent from both the active layer thickness and the p-spray and p-stop isolation. This would advise against the use of punch-through structures or it would at least suggest their strong miniaturization in order to confine their effects within the smallest possible area of the sensor.

V. Performance of thin 3D sensors

The MIP-MPV as a function of the bias voltage, measured before irradiation, is shown in Fig. 9 for the standard 3D sensors (100×150 μm^2 pixel size), and in Fig. 10 for small pitch 3D sensors (25×100 μm^2 and 50×50 μm^2 pixel sizes).

The collected charge is compatible, within the uncertainties, with that of planar sensors with the same active layer thickness.

The corresponding MIP signal spectra measured before irradiation are reported in Fig. 11 for the standard pitch 3D sensors at a bias voltage of 40 V and in Fig. 12 for the small pitch 3D sensors at a bias voltage of 50 V. The small ridge on the left-hand side of the two Landau function peaks of Fig. 12 is mainly due to the charge-sharing effects with the surrounding pixel cells which are not read out.

The measured particle detection efficiency at a threshold of about 2000 electrons is greater than 99% for orthogonally incident particles (Table I), even though an unavoidable degradation of the efficiency is observed in correspondence to the junction and Ohmic columns. Complete uniformity of the efficiency can be obtained by tilting the sensors by 5° with respect to the incident particles.

TABLE I
Efficiency for standard, 100×150 μm^2 pixel size, 3D sensors as a function of the angle of the incident particle.

Angle (degree)	Efficiency 3E (%)	Efficiency 2E (%)
0	99.27	99.45
5	99.77	99.85
10	99.88	99.87

Unfortunately, we are not able to show the MIP-MPV as a function of the bias voltage for irradiated 3D sensors because of unreliable calibration of the readout chip due to radiation damage. We believe that during the irradiation campaign of these 3D detectors, the center of the proton beam was slightly offset with respect to the center of the sensor, hence damaging

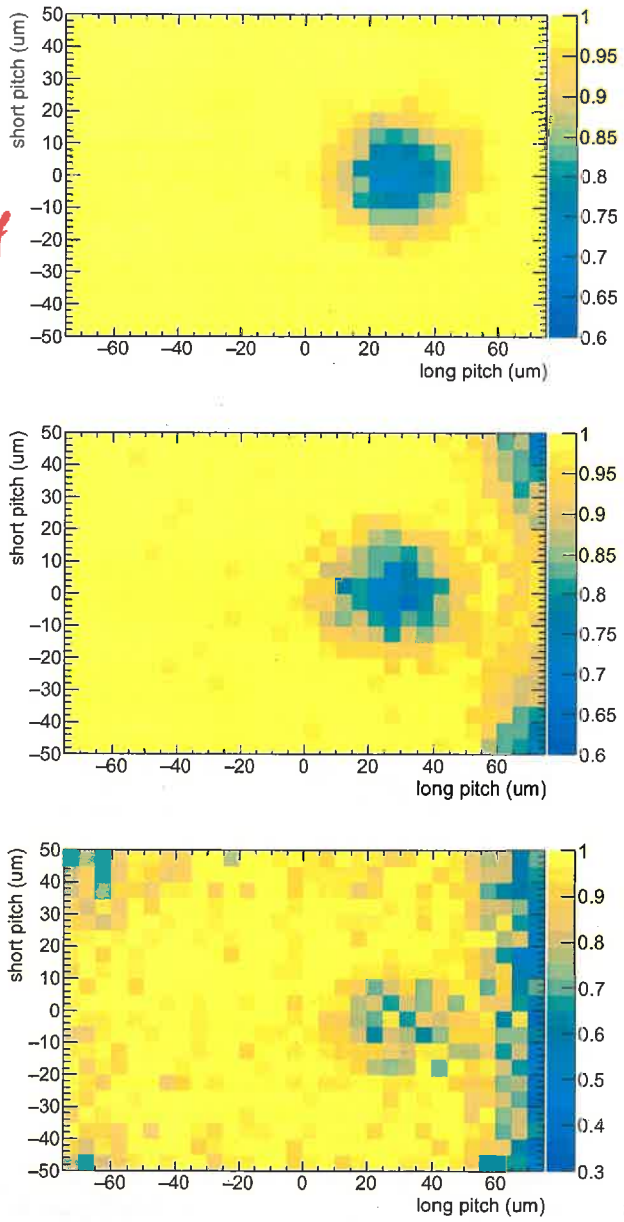

Fig. 8. Maps of the detection efficiency within the pixel cells of the most irradiated sensor (Fig. 6) before the irradiation at bias voltages of 40 V (top plot) and 150 V (center plot), and, once irradiated up to $\sim 5 \times 10^{15}$ n_{eq}/cm^2, at a bias of 650 V (bottom plot). The efficiency clearly results affected by the punch-through and its bias grid.

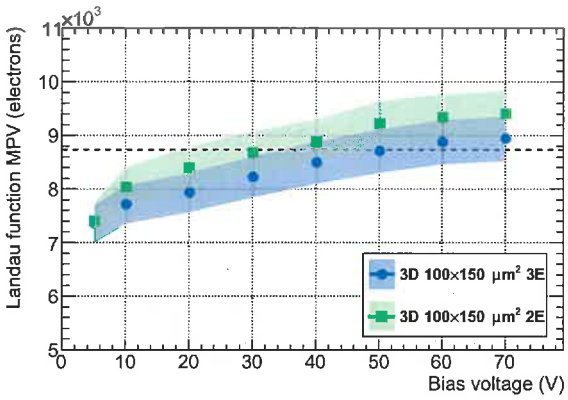

Fig. 9. MIP-MPV as a function of the bias voltage for two non-irradiated 3D sensors, one with two junction columns (2E), the other with three (3E). The sensor thickness is 130 μm and the pixel size is 100 × 150 μm^2. The horizontal dashed line indicates the expected value, while the dashed lines show the measurement uncertainties.

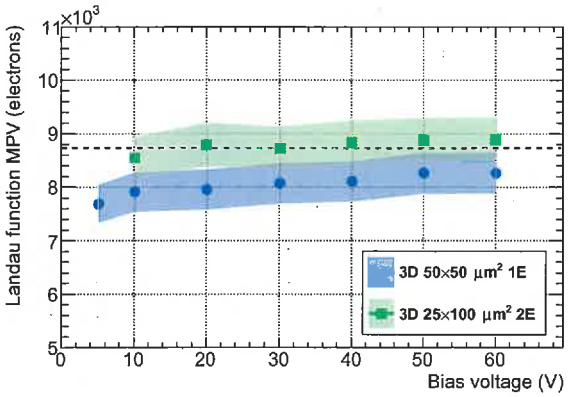

Fig. 10. MIP-MPV as a function of the bias voltage for non-irradiated 3D sensors with 50 × 50 μm^2 (1E) and 25 × 100 μm^2 (2E) pixel size. The dashed line indicates the expected value, while the dashed lines reflect the measurement uncertainties.

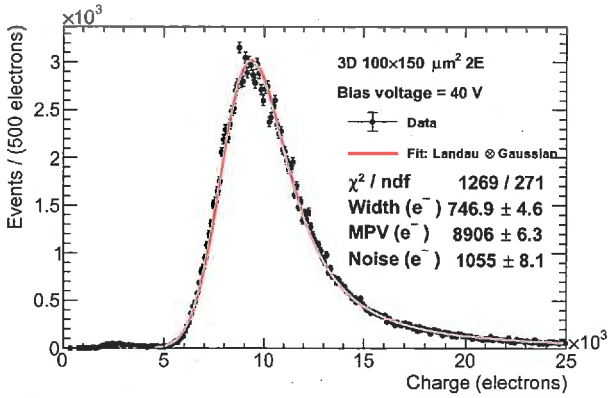

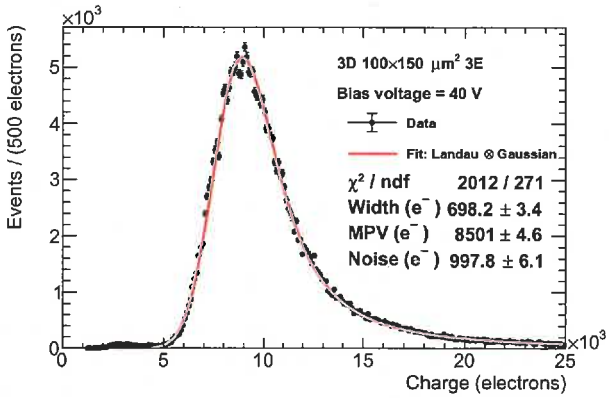

Fig. 11. The MIP signal spectra measured with 100 × 150 μm^2 3D sensors before irradiation. The top plot refers to a two junction electrodes sensor (2E), while the second to a three junction electrodes sensor (3E). The plots correspond to the two measurements of Fig. 9 at a bias voltage of 40 V.

the periphery of the readout chip which is responsible for the digitization of the pulse height. Nevertheless, we measured their detection efficiency as a function of the bias voltage as reported in Fig. 13 for orthogonally incident particles. At a bias voltage of 200 V the most irradiated (~ 5 × 10^{15} n_{eq}/cm^2) sensor reaches 96% efficiency at a threshold of about 3000 electrons. This performance is certainly excellent given the rather high threshold set. By lowering the threshold to about 2000 electrons we should indeed recover the full detection efficiency.

VI. Conclusion

The INFN joint ATLAS-CMS Pixel R&D group has developed in collaboration with FBK the first prototypes of new silicon pixel sensors capable to resist the very high radiation fluences expected in HL-LHC. Both thin planar and 3D sensors have been produced. First beam tests of these prototypes have been carried out using the readout chip presently in use in CMS, PSI46 digital. Their measured performance is excellent up to the maximal irradiation fluence tolerated by the employed readout chips, ~ 5 × 10^{15} n_{eq}/cm^2. Both the thinner planar sensors and the 3D 3E sensors reach a particle detection efficiency of about 96% at a rather high threshold of ~ 3000 electrons and a bias voltage of 650 V and 200 V, respectively. A noticeable improvement of the measured performance is expected by lowering the thresholds at the level of 1000 electrons. A further improvement of the performance of the 3D sensors should be achieved exploiting the smaller distance between the electrodes of the finer pitch 3D sensors, as in case of 25 × 100 μm^2 and 50 × 50 μm^2 pixel size. To finally qualify these prototypes for HL-LHC a much more radiation resistant readout chip is required. The first prototype of the RD53 readout chip will be available soon. It will allow for operation at the expected HL-LHC fluence and at a threshold close to 1000 electrons.

Acknowledgment

This work was supported by the Italian National Institute for Nuclear Physics (INFN), projects ATLAS, CMS, RD-FASE2

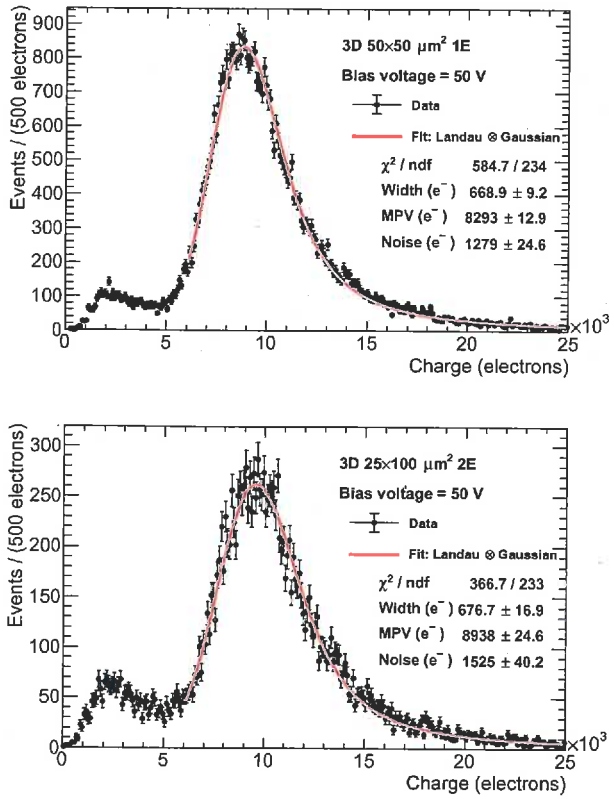

Fig. 12. The MIP signal spectra measured, before irradiation, with a 50 × 50 μm^2 3D, type 1E, sensor (top plot) and with a 25 × 100 μm^2 3D, type 2E, sensor (bottom plot). The spectra correspond to the two measurements reported in Fig. 10 at 50 V bias voltage.

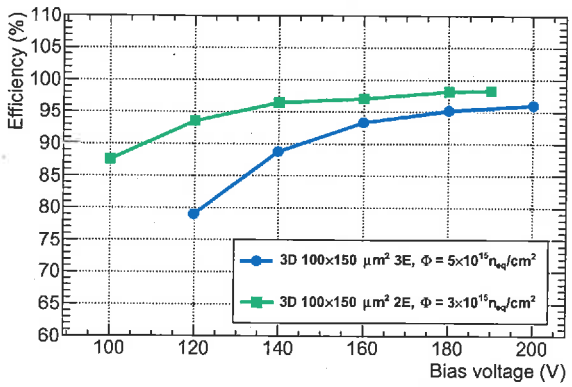

Fig. 13. Efficiency as a function of the bias voltage for irradiated 3D sensors. The threshold of the most irradiated sensor is ~ 3000 electrons, while for the other sensor is ~ 2000 electrons.

(CSN1), and by the European Union's Horizon 2020 Research and Innovation program under Grant Agreement no. 654168.

REFERENCES

[1] L. Evans, and P. Bryant (editors), JINST **3** (2008) S08001.
[2] The ATLAS Collaboration, JINST **3** (2008) S08003.
[3] The CMS Collaboration, JINST **3** (2008) S08004.
[4] C. DaVia et al., Nucl. Instrum. Methods Phys. Res. A **603** (2009) 319.
[5] CMS Collaboration, "The phase-2 upgrade of the CMS tracker," CERN-LHCC-2017-009 CMS-TDR-014.
[6] IceMos Technology (Belfast, Ireland) web site: http://www.icemostech.com.
[7] H.C. Kaestli, Nucl. Instrum. Methods Phys. Res. A **731** (2013) 88.
[8] G.F. Dalla Betta et al., Nucl. Instrum. Methods Phys. Res. A **824** (2016) 386.
[9] H.Bichsel, Review of Modern Physics **60** (1988) 663.
[10] G.F. Dalla Betta et al., Proceedings of Science (Vertex 2016) **028**.
[11] S. Kwan et al., Nucl. Instrum. Methods Phys. Res. A **811** (2016) 162.
[12] Los Alamos irradiation facility web site: https://www.lanl.gov.
[13] CERN PS-IRRAD Proton Facility web site: https://ps-irrad.web.cern.ch.
[14] L. Gaioni (on behalf the RD53 Collaboration), *"Test results and prospects for RD53A, a large scale 65 nm CMOS chip for pixel readout at the HL-LHC,"* NIM-A (2018) in press (web version: https://doi.org/10.1016/j.nima.2018.11.107).
[15] H.J. Hendrik, doctoral thesis, "Search for supersymmetry with multiple charged leptons at $\sqrt{s} = 13$ TeV with CMS and radiation tolerance of the readout chip for the phase I upgrade of the pixel detector," https://doi.org/10.3929/ethz-b-000182698.